

## Characterization of Mechanically Alloyed Polymer Blends for Selective Laser Sintering

**Julie P. Martin and Dr. Ronald G. Kander**

*Department of Materials Science and Engineering, Virginia Polytechnic Institute and State University, Blacksburg, VA 24061-0237, USA*

Cryogenic mechanical alloying (CMA) is presented in this work as an effective technique for creating materials for selective laser sintering (SLS) applications. CMA offers a solid state method for creating micro-composites consisting of finely dispersed phases, which can then be selectively laser sintered into parts containing co-continuous phases. Particle size and shape, microstructure, and melting characteristics of mechanically alloyed particles are discussed in terms of applications to the SLS process. The characteristics of several model polymer blend systems are investigated using scanning electron microscopy, light scattering particle size analysis, and differential scanning calorimetry. Although only polymer/polymer blend particles are studied here, the CMA process is also a viable technique for creating SLS powders using ceramics or metals.

### INTRODUCTION AND BACKGROUND

Conventional polymer blending techniques such as solution and melt blending require high temperatures, solutions, or compatibilizers. However, a solid state processing technique called cryogenic mechanical alloying (CMA) can be used to blend polymers in powder form without the need for solvents, compatibilizers, or a common processing temperature window. Mechanical alloying (MA) is beneficial for blending immiscible polymers and creating novel morphologies with sub-micron phase domains. Traditional thermal blending techniques such as extrusion and injection molding require the polymers to flow on a macroscopic level. However, polymer powders blended via MA can be selectively laser sintered into useful part geometries. This allows much of the refined microstructure created during mechanical alloying to be retained in the final part since no macroscopic flow is required during the laser sintering step<sup>1,2</sup>.

Mechanical milling (one component) and mechanical alloying (two or more components) are techniques which were originally developed for solid state processing of metals in the late 1960s. Mechanical alloying is currently widely used in the metals industry for producing composite metal powders with fine microstructures. During mechanical alloying, a ball mill is used to produce alloyed powders. The starting materials (in powder or pellet form) are placed in the ball mill vial with two or more metallic or ceramic balls (Figure 1).

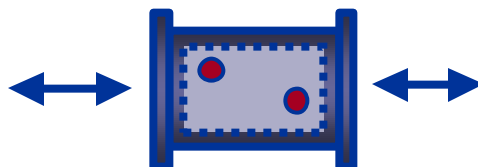


**Figure 1.** Schematic of vibratory ball mill vial and balls<sup>3</sup>.

In a vibratory ball mill, high energy impacts between the balls and the material occur when the mill's motor vigorously shakes the vial, trapping material between the balls (and between the balls and the vial walls) with each agitation (Figure 2).

As CMA occurs, the particles are repeatedly fractured, deformed, and fused together. This process of repeated fracturing and cold-welding causes a refinement in microstructure with milling time. The result is a two-phase lamellar or plate-like microstructure with an interlamellar distance dependent on processing time<sup>4</sup> (Figure 3). Other processing parameters which affect the composite microstructure include the energy input, which can be controlled by manipulating the ratio of the total ball mass to the powder mass (charge ratio), milling temperature, ball mill design, and number and size of balls used. The milling temperature can be critical because of its effect on both the material ductility and thermally-aided diffusion across interfaces.

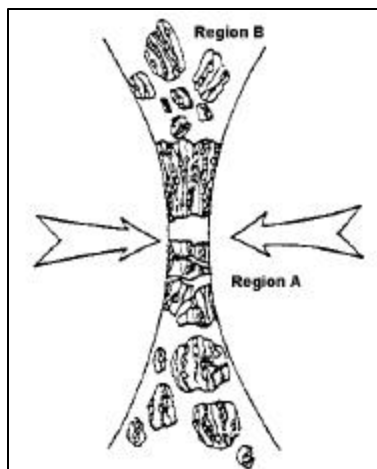


**Figure 2.** High energy ball-powder-ball collision, resulting in welding (Region B), extensional flow, and fracture (Region A)<sup>3</sup>.

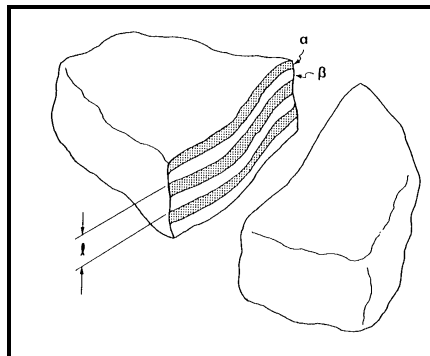


**Figure 3.** Two-phase lamellar microstructure of powder particles produced by mechanical alloying<sup>5</sup>.

Because CMA can combine immiscible materials, there are virtually unlimited numbers of polymeric systems that can be blended via mechanical alloying. Despite this fact, only a few researchers have applied this technique to blending polymers. To date, the field of mechanically alloyed polymers has been explored to a moderate degree at best. This work aims to investigate CMA as a process for producing desirable materials for the SLS process. Although polymer-polymer systems are studied here, this process can be applied to ceramics and metals as well.

The field of CMA polymers is currently lacking a systematic understanding of how variations in processing parameters affect the resultant microstructure of the alloyed powders and post-processed parts. Understanding these relationships are crucial because the microstructure dictates the mechanical properties of the material. Therefore, it is important to understand how mechanical milling and alloying change a system's microstructure in order to engineer a microstructure based on desired macroscopic properties. This work investigates processing-microstructure relationships of mechanically alloyed polymeric micro-composites. While demonstration systems are studied here, a better understanding of how CMA affects these systems will lead to development of SLS materials. A vibratory ball mill was

used to produce polymeric blends, and several techniques were used to investigate the effects of the mechanical alloying process on these materials.

## EXPERIMENTAL PROCEDURE

### *Cryogenic Mechanical Alloying Process*

A novel laboratory-scale vibratory ball mill was designed and built by a colleague at Virginia Tech<sup>2</sup>. When operated at cryogenic temperatures, the vial is continuously exposed to a liquid nitrogen bath throughout the milling process. The ball mill can also be operated at ambient temperature by omitting the liquid nitrogen. The milling vial and balls (shown schematically in Figure 1) are stainless steel; the vial has an inside diameter of 3 inches, and the diameter of each ball is 0.8125 inches. A schematic of the ball mill is shown in Figure 4.

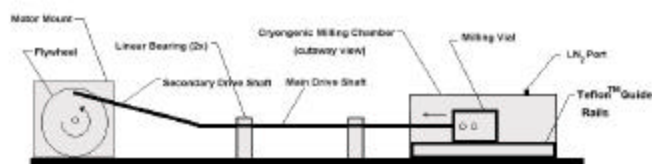


**Figure 4.** Vibratory ball mill with both ambient and cryogenic capabilities designed at Virginia Tech<sup>2</sup>.

### *Demonstration Systems*

Mechanically alloyed micro-composites consisting of DTM Duraform™ Polyamide (nylon 12) were blended with polypropylene (PP), Victrex™ poly(ether ether ketone) (PEEK) and DTM polycarbonate (PC). Blends were produced from resins in powder form in a 50/50 volume percent ratio. The powders were cryogenically mechanically alloyed for 1 hour. In addition individual components were cryogenically mechanically milled (CMM) at the same conditions.

### *Differential Scanning Calorimetry (DSC)*

Thermal analysis was performed on as-received nylon 12 powders as well as the CMA blends. A Perkin Elmer DSC7 was used to investigate crystallization and melt properties of the powders. Powders were heated from room temperature to 225°C at a rate of 10°/minute, held in the melt for five minutes, then cooled at a rate of 10°/minute. Glass transition, melting, and recrystallization temperatures were determined.

### *Scanning Electron Microscopy (SEM)*

An International Scientific Instruments SX-40 scanning electron microscope with an accelerating voltage of 20kV was used to image the topology of CMM powders as well as unprocessed powders. The powders were sputtered with gold prior to imaging.

### Particle Size Analysis

A Horiba LA-700 Laser Scattering Particle Size Distribution Analyzer was used to obtain particle size distributions and average particle sizes for CMA blends, CMM individual components and as-received materials. Powders were dispersed in ethanol for analysis.

## RESULTS AND DISCUSSION

There are several important material properties to consider when developing materials for the SLS process. These properties include particle size and shape, particle melting characteristics, and particle microstructure. The techniques used in this ongoing study aim to address each of these issues.

### Particle Size Characterization

Median and mean particle sizes averaged from three runs are shown in Table 1 below. Measurements of distribution breadth such as population standard deviation and dispersity index (second moment/first moment) are also shown along with a 95% range, which indicates the size range within which 95% of the particles fall. All CMM samples were cryogenically mechanically milled for 1 hour, all CMA samples were cryogenically mechanically alloyed for 1 hour.

<i>Material</i>	<i>Mean (<math>\mu\text{m}</math>)</i>	<i>Median Particle Size (<math>\mu\text{m}</math>)</i>	<i>Population Std. Deviation (<math>\mu\text{m}</math>)</i>	<i>Dispersity Index</i>	<i>95% of Particles fall within range: (<math>\mu\text{m}</math>)</i>
As-Received Nylon 12	46.50 - 1.18	39.98 - 0.76	40.7	1.3	9.87-95.50
As-Received PEEK	42.6 - 0.26	46.58 - 0.57	41.6	1.5	0.30-144.0
As-Received PC	85.3 - 4.37	79.40 - 4.44	39.2	1.2	35.63-150.00
As-Received PP	40.93 - 0.71	34.34 - 0.43	41.7	1.3	9.49-88.88
CMM Nylon 12	32.67 - 0.98	26.97 - 0.58	44.4	1.6	2.34-83.27
CMM PC	91.07 - 1.46	83.03 - 1.41	47.7	1.2	13.56-172.7
CMM PP	30.87 - 5.32	27.09 - 0.52	43.6	1.4	3.51-84.70
CMA PP/Nylon12	30.53 - 0.72	28.26 - 1.16	44.7	1.3	3.34-82.36
CMA PC/Nylon 12	30.53 - 1.15	37.60 - 1.17	44.8	1.6	3.51-138.13
CMA PEEK/Nylon 12	39.47 - 2.0	33.48 - 2.86	43.3	1.5	2.18-114.00

**Table 2.** Particle size distribution results.

CMM and CMA generally decreases the overall particle size and increases the dispersity index, although the mean and median values for CMM PC were actually higher than the as-received PC. The lower limits of the 95% range may pose problems for SLS, as extremely small particles may not sinter well due to inefficient packing and relatively large surface area per unit volume. Further analysis of particle distributions is necessary for a better understanding of how CMA affects particle size in relationship to the SLS process.

### *Particle Shape Characterization*

The effects of the CMM process can be seen in both the shape and topology of the powder particles (Figures 5-9). When nylon 12 is CMA with another polymer such as PP (Figure 9), the effects of the cold welding and fracturing mechanisms of the CMA process are evident. The layered topology of the CMA blend means that each particle now contains both nylon 12 and PP, but the microstructure of these particles cannot be characterized using SEM. The change in both size distributions and shape have implications for powder handling and packing in the SLS powder bed, as well as in the sintering step itself.

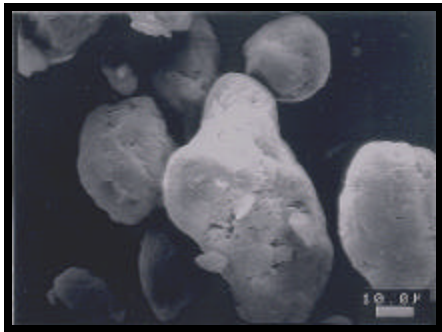


**Figure 5.** As-received nylon 12.

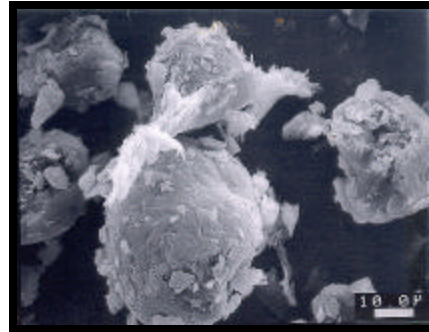


**Figure 6.** Nylon 12 CMM 1 hour.



**Figure 7.** As-received PP.

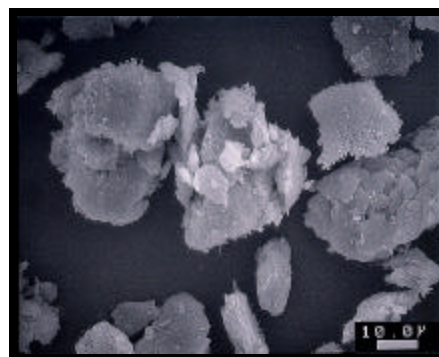


**Figure 8.** PP CMM 1 hour.

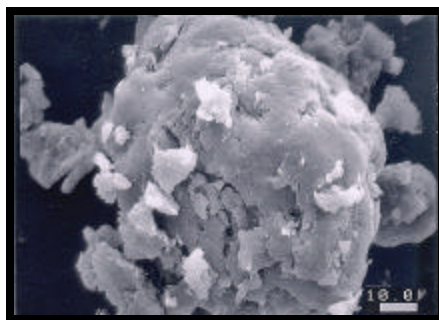


**Figure 9.** Nylon 12/PP CMA 1 hour.

## Particle Thermal Characteristics

The melting and recrystallization characteristics of SLS materials have implications for laser power and speed necessary to sinter the particles. In addition, once the particles have been melted by the laser, the temperature/speed at which they recrystallize can affect the thermal stresses present in the finished part. It is desirable for one layer to stay soft during a given laser scan so that when the next layer is added, the powder “sticks” to the previous layer and residual stresses are minimized. Therefore, it is desirable to use a system that has a large difference in melting and recrystallization temperatures to maximize the time between the laser contact and recrystallization. The absolute melting ( $T_m$ ) and/or softening temperature ( $T_g$ ) is also important, as it contributes to the laser power necessary for SLS processing. Here, the thermal behavior of the pure nylon 12 component is compared to the thermal behavior of nylon 12 present in the CMA blends. The DSC thermograms presented in Figures 10-13 show the thermal behavior of nylon 12 as well as blends of nylon 12/PP, nylon 12/PC, and nylon 12/PEEK. The red line is data collected as the as-received or CMA powder sample is heated; the blue line is the data collected as the sample is cooled from the melt. The endothermic melting transition is present in the heat scans, while the exothermic recrystallization transitions are visible in the cooling scans.

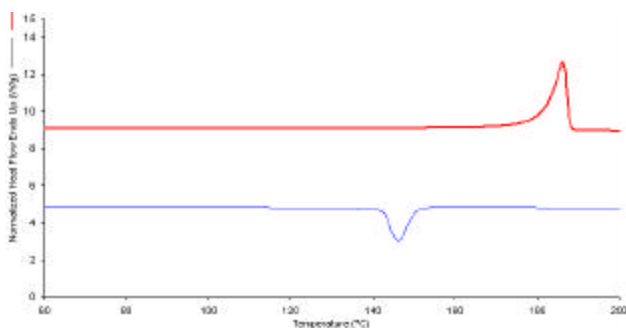


**Figure 10.** As-received nylon 12.

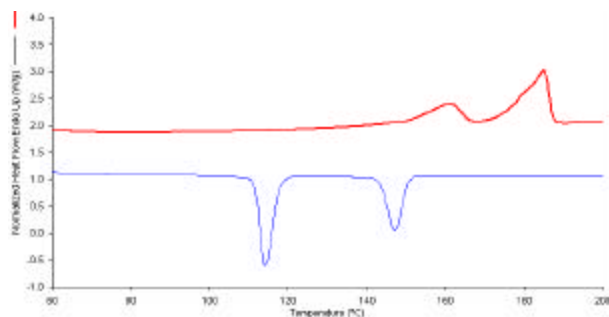


**Figure 11.** Nylon 12/PP CMA 1 hour.

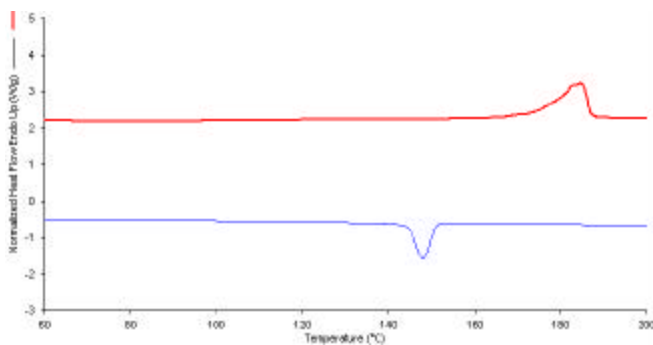


**Figure 12.** Nylon 12/PC CMA 1 hour.

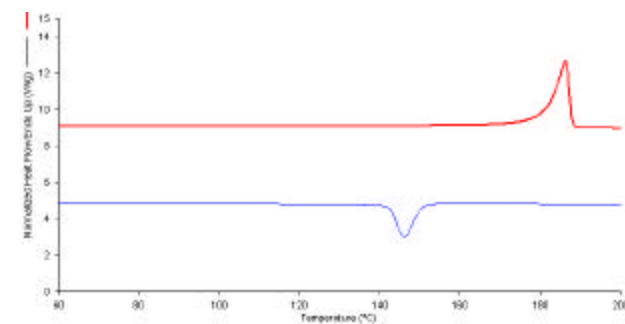


**Figure 13.** Nylon 12/PEEK CMA 1 hour.

The CMA blends used in this work demonstrate the thermal behavior of several categories of systems. The nylon 12/PP system is one where both phases co-melt during SLS. In the nylon 12/PC system, the PC phase is amorphous, but is above its  $T_g$  in the melting range of nylon 12 ( $T_g^{PC}=145^\circ\text{C}$ ). In the nylon 12/PEEK system, the PEEK phase melts at a much higher temperature than the nylon 12 phase ( $T_m^{PEEK}=345^\circ\text{C}$ ). During selective laser sintering of the nylon 12/PEEK blend near the  $T_m$  of the nylon

12 phase, the PEEK serves as a reinforcement. Thermal properties of the nylon as well as the other blend component are summarized in Table 2 below.

	Nylon 12	Nylon 12/PP Blend	Nylon 12/PC Blend	Nylon 12/PEEK Blend
$T_m^{\text{nylon}}$	186 °C	185 °C	185 °C	185 °C
<b>Melt onset</b>	182 °C	176 °C	174 °C	178 °C
<b>Melt end</b>	188 °C	187 °C	187 °C	187 °C
$\Delta H_m^{\text{nylon}}$	119 J/g	44 J/g	48 J/g	51 J/g
$T_m^{\text{component}}$	-	161 °C	-	N/A
<b>Melt onset</b>	-	150 °C	-	N/A
<b>Melt end</b>	-	166 °C	-	N/A
$T_c^{\text{nylon}}$	146 °C	147 °C	150 °C	148 °C
<b><math>T_c</math> onset</b>	150 °C	151 °C	153 °C	151 °C
<b><math>T_c</math> end</b>	143 °C	147 °C	147 °C	144 °C
$T_c^{\text{component}}$	-	114 °C	-	N/A
<b><math>T_c</math> onset</b>	-	118 °C	-	N/A
<b><math>T_c</math> end</b>	-	112 °C	-	N/A
$\Delta H_c^{\text{nylon}}$	54 J/g	28 J/g	24 J/g	24 J/g

**Table 3.** Thermal properties of nylon 12 and its CMA blends.

These DSC samples were heated to a temperature of 225°C, so the PEEK melting and recrystallization temperatures are not shown. The heat of melting ( $\Delta H_m^{\text{nylon}}$ ) and heat of recrystallization ( $\Delta H_c^{\text{nylon}}$ ) for nylon 12 is approximately half that of the pure component. This is because the blends consist of 50/50 by volume of each component. The onset and end of melting occurs at approximately the same temperature in all the blends. The presence of another phase slightly lowers the onset of melting compared with that of pure nylon 12. The onset and end of crystallization occurs at approximately the same temperature in the pure component and in the blends. Thus, the SLS processing temperature window ( $T_m - T_c$ ) remains approximately the same for the CMA blends and pure nylon 12.

### *Particle Microstructure*

The characterization of CMA particle microstructure presents many challenges, and several techniques have been attempted to date with limited results. Atomic force microscopy and transmission electron microscopy have yielded images, but the structure seen is believed to be an artifact of the sample preparation rather than the CMA process. Current efforts are focused on using chemical differences of the two CMA phases to determine the size of the phase domains present in the CMA blend particles. The microstructure of the CMA powders will be investigated as well as the microstructure of the selectively laser sintered parts so that processing-structure-properties relationships can be established

### ACKNOWLEDGMENTS

The authors gratefully acknowledge the support of DTM Corporation in Austin, TX. The authors also thank Jeff Schultz at Virginia Tech for assistance with the ball mill.

---

<sup>1</sup>Pan, W.J.D. and Shaw, J., *Journal of Applied Polymer Science*, **56**, 1995, 557-566.

<sup>2</sup>Schultz, J. P., Kander, R.G., and Suchicital, C.T.A., *Solid Freeform Fabrication Proceedings*, 1999, 311-317.

<sup>3</sup>Gilman, P. S. and Benjamin, J. S., *Annual Review in Materials Science*, **13**,1983, 279-300.

<sup>4</sup>Farrell, M.P., Kander, R.G., and Aning, A.O., *Journal of Materials Synthesis and Processing*, **4**,1996,151-161.

<sup>5</sup>Maurice, D.R. and Courtney, T.H., *Metallurgical Transactions A*, **21A**, 1990, 289-303.